Calcareous nannofossil communities during Late Triassic Mass Extinction and Early Jurassic recovery in the NW Tethys: evidence from Slovakia, Western Carpathians

KATARÍNA HOLCOVÁ, MATIC RIFL, and JOZEF MICHALÍK

Holcová, K., Rifl, M., and Michalík, J. 2024. Calcareous nannofossil communities during Late Triassic Mass Extinction and Early Jurassic recovery in the NW Tethys: evidence from Slovakia, Western Carpathians. *Acta Palaeontologica Polonica* 69 (3): 485–500.

The first calcareous nannoplankton extinction and recovery close to the Triassic/Jurassic boundary (TJB) were studied in two Tatra Mountains sections of Kardolína and Furkaska. The studied sediments were deposited in an intra-shelf depression of the Tethyan shelf (the Zliechov Basin). Rare nannofossil assemblages were discovered in both sections. Rhaetian nannofossils are characterized by the dominance of *Prinsiosphaera triassica* and by episodic increases in the abundance of small-sized coccoliths. Coccoliths belonging to *Calyculus*? *kardolinae* sp. nov. were found on tops of the bedding planes. Triassic index species *Eoconusphaera* aff. *hallstattensis* was also recovered, it is rare though, probably due to the marginal or relatively high-latitudinal position of the area. The uppermost Triassic is characterized by a significant reduction in nannofossil abundance accompanied by the presence of organic matter in the rock, which was significant especially in the Kardolína section. The signal of the last occurrence of *Prinsiosphaera triassica* is overwritten by the reworking of Upper Triassic material into Jurassic strata within the boundary clay interval. The presence of representatives of Watznaueriaceae in the Jurassic Kopieniec Formation is surprising and might indicate hiatus in the TJB in the studied sections. We are also presenting the results of a newly developed method for the extraction of calcareous nannofossils from indurated rocks.

Key words: Calcareous nannofossils, biostratigraphy, taphonomy, Rheatian, Hettangian, Tatra Mountains.

Katarína Holcová [katarina.holcova@natur.cuni.cz; ORCID: https://orcid.org/0000-0002-8371-3510] and Matic Rifl [riflmatic@gmail.com; ORCID: https://orcid.org/0000-0003-4816-9502], Institute of Geology and Palaeontology, Faculty of Sciences, Charles University, Albertov 6, Praha 2, Czech Republic.
Jozef Michalík [michalikuvz@gmail.com; ORCID: https://orcid.org/0000-0003-2541-0666] Earth Science Institute, Slovak Academy of Science, Dúbravská 9, P.O. Box 109, 84005 Bratislava, Slovakia.

Received 8 August 2023, accepted 6 May 2024, published online 27 September 2024.

Introduction

The Late Triassic Mass Extinction event was the second largest extinction since the Cambrian, affecting both the terrestrial and marine ecosystems (Alroy 2010; Blackburn et al. 2013; Dunhill et al. 2018). It was evoked by the activity of the Central Atlantic Magmatic Province, causing global warming, sea-level changes, ocean anoxia, and ocean acidification (Hallam 1981; Hallam and Wignall 2000; Wignall 2001; Hautmann 2004; Marzoli et al. 2004, 2008, 2011; McElwain et al. 2007; Whiteside et al. 2007, 2010; Deenen et al. 2010; Ruhl et al. 2011; Bonis and Kürschner 2012; Jaraula et al. 2013; Lindström et al. 2017; Tetsuji et al. 2022). Radiometric dating of the two events (eruptions of the Central Atlantic Magmatic Province and the Late Triassic Mass Extinction) yielded identical ages of ~201.6 Ma (Blackburn et al. 2013), supporting the coincidence of these processes (Hautmann et al. 2008). Moreover, the Late Triassic Mass Extinction level corresponds to the initial $\delta^{13}C_{org}$ excursion (the Initial Carbon Isotope Event = ICIE), which occurred 120 ky before the end of the Triassic. The events were associated with a major regression during enhanced earthquake activity in Europe (Lindström et al. 2017).

Calcareous nannoplankton belongs to the most significant group of calcifiers (Bown et al. 1991; Erba 2006), responding to changes in seawater chemistry with a high sensitivity (Stanley 2008). According to Stanley (2006), the drop of seawater Mg/Ca ratios caused individual coccoliths to become less massive and less prone to fossilization. Subsequent short-time rise in the Mg/Ca value of

seawater around the TJB might have influenced biomineralization processes of these calcifiers (Lowenstein et al. 2001). Another widely known feature is the selective diagenetic loss, especially of fragile specimens (Bown 1998; Hillebrandt et al. 2013). Experiments showed that the leading factor triggering coccolith dissolution is the pH decrease (already below 7.8; Hassenkam et al. 2011). The pore water chemistry (including its pH) that influences the early diagenetic environment is controlled by multiple factors, ocean water pH being one of them. Therefore, a rapid acidification of the ocean water around the TJB can cause diagenetic alteration of the calcareous nannoplankton abundance.

The evolution of calcareous nannoplankton assemblages around the TJB was studied in Britain, Germany, Austria, Italy, North America, and also on the Southern Hemisphere (Jafar 1983; Bown 1987, 1998; Bralower et al. 1991; Preto et al. 2012, 2013a, b; Hillebrandt et al. 2013; Demangel et al. 2020). However, the evolutionary history of nannoplankton around the TJB interval and its recovery during the early Hettangian are still poorly known (Bottini et al. 2016).

This study is focused on the documentation of changes in the calcareous nannofossil assemblages around the TJB in a marginal intra-shelf basin of the NW Tethys. The evolution of calcareous nannoplankton assemblages around the TJB interval is described in view of the palynological, sedimentological, and geochemical changes defined by the recently studied multiproxies (Lintnerová et al. 2013; Michalík et al. 2007, 2010).

Institutional abbreviations.—CHMHZ, Chlupáč Museum of Earth History, Charles University, Prague, Czech Republic.

Other abbreviations.—FO, the first occurrence; ICIE, the Initial Carbon Isotope Event; LO, the last occurrence; TJB, the Triassic/Jurassic boundary.

Nomenclatural acts.—This published work and the nomenclatural acts it contains have been registered in IFPNI PFN003347

Geological setting

During the latest Triassic, the Austro-Alpine–Central Carpathian block became detached from the European shelf by the Penninic rifting (Kuss 1983; Michalík 1993, 1994). Inside this block, a small pull-apart Zliechov Basin was formed, 300 km in length and 100 km in width. A shallow marine carbonate sequence (Fatra Formation) was deposited transgressively on terrestrial Carpathian Keuper deposits (Stur 1859; Michalík 1973, 1974, 1977, 1978, 2007). Storms and sea-level fluctuations combined with a slow (22–38 mm/kyr) subsidence rate hampered the formation of coral, sponge, algal and hydrozoan patch-reefs on the edge of the carbonate ramp (Michalík 1982; Tomašových 2004; Vďačný et al. 2019). The slope of the ramp was facing toward a deeper, dysoxic bottom without benthic fauna (similarly as in the

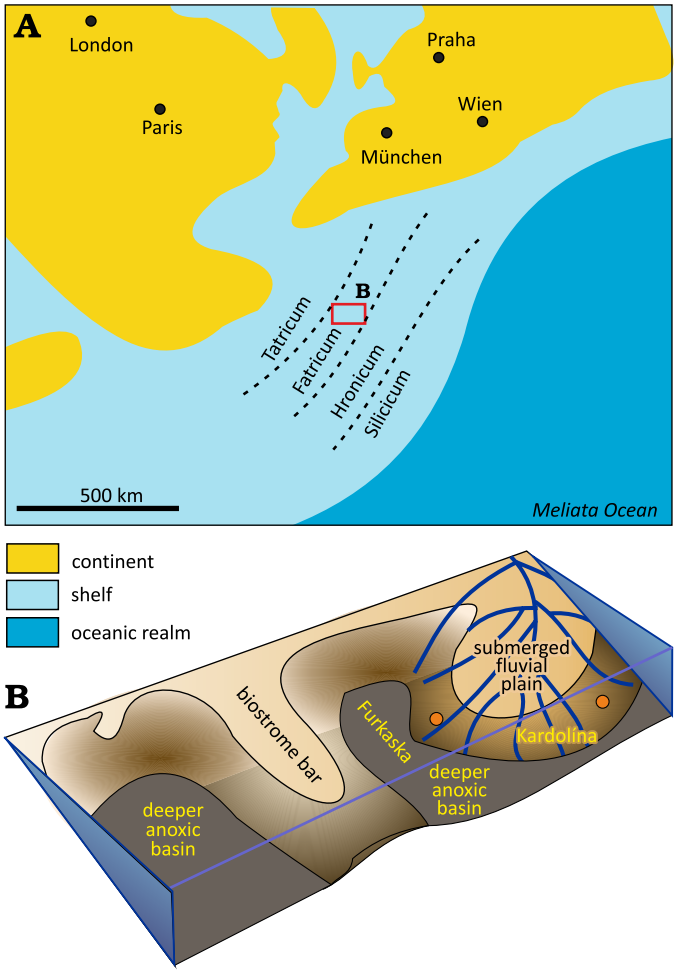

Fig. 1. Paleogeographic position of the studied sections within the Late Triassic Tethys. **A**. Overall paleogeographical situation. **B**. A close-up view of the Zliechov Basin with the locations of the study sections. Modified after Michalík et al. (2007).

Alpine Kössen Basin; Kuss 1983; Fig. 1). Terrigenous clastic component in these Upper Triassic limestones of the Fatra Fm. is generally low (Vďačný et al. 2019). Benthic associations were dominated by brachiopods *Rhaetina gregaria* (Michalík 1975, 1978, 1980) and bivalves (e.g., *Placunopsis alpina* or *Rhaetavicula contorta*; Michalík and Jendrejáková 1978; Michalík 1978). The thickness of the Fatra Formation is 25–116 m.

Sedimentary rocks of the Fatra Formation are topped by a sharp contact, being overlain by marine shales of the Hettangian Kopieniec Formation (Goetel 1917; Gaździcki et al. 1979; Tomašových and Michalík 2000) consisting of brown claystones with sandstone and limestone intercalations. Light-coloured quartz sandstone contains infrequent tourmaline grains and thin muscovite flakes (Gaździcki et al. 1979). It is locally replaced by red siltstone, comparable with the Schattwald Beds of the Eastern Alps (Borza et al. 1980). The lower Hettangian Calliphyllum Zone, partially correlated with the Planorbis Zone, has been reported from three localities; ammonites *Psiloceras psilonotum* and *Caloceras* cf. *torus* were found in the uppermost part of the "basal clastic member",

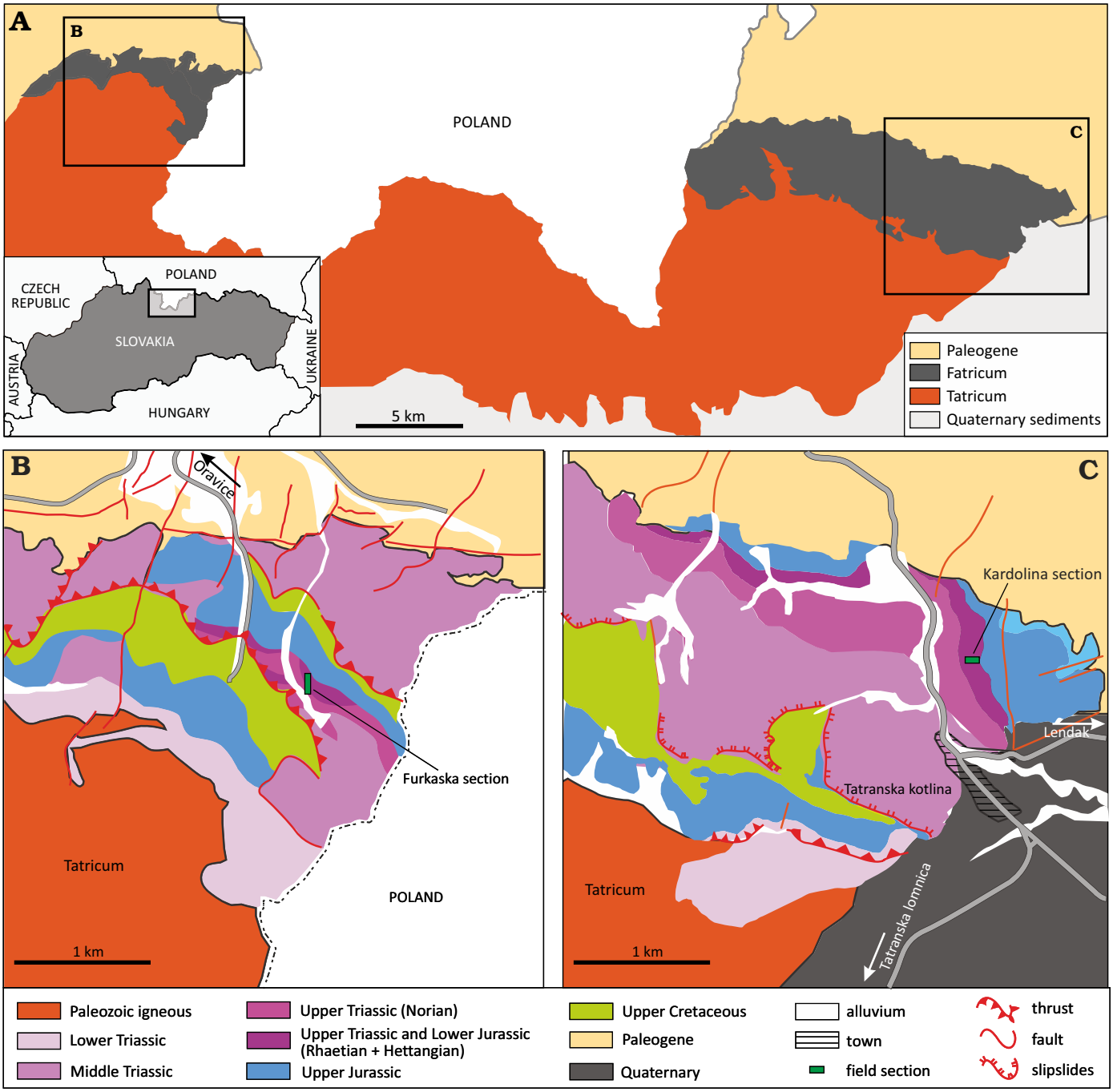

Fig. 2. Map of Slovakia with study area indicated (inset). **A**. Geological map of the Slovakian part of Tatra Mountains showing the positionss of the Furkaska (**B**) and Kardolína (**C**) sections (modified from https://apl.geology.sk/).

ammonites of middle and late Hettangian age (from Liassicus and Angulata zones) occur sporadically in the middle of the formation (Rakús 1975, 1993, 2003; Gaździcki et al. 1979). Moreover, a detailed zonation of the Triassic/Jurassic boundary interval of the Zliechov Basin is based on foraminifera (Michalík et al. 2007). The TJB can be also determined from palynomorphs (Ruckwied and Götz 2009).

The study of the TJB interval in the Kardolína and Furkaska sections resulted in a recognition of several events, which characterize the paleoenvironment of the Triassic/Jurassic boundary interval in the study area. The negative $\delta^{13}C_{org}$ excursion correlated with the ICIE and pre-dating the TJB by 120 kyr was recorded in Beds 100–102 of the Kardolína section and in Beds 409–414 of the Furkaska section (Tanner 2010; Michalík et al. 2007; Fig. 3). This $\delta^{13}C_{org}$ excursion can be correlated with a decrease in benthic fauna diversity (Michalík et al. 2007, 2010, 2013).

Two beds composed of calcified microspheres (spherule beds) are situated in an interval with variegated values of $\delta^{13}C_{inorg}$ (Beds 48–53 in the Kardolína section and

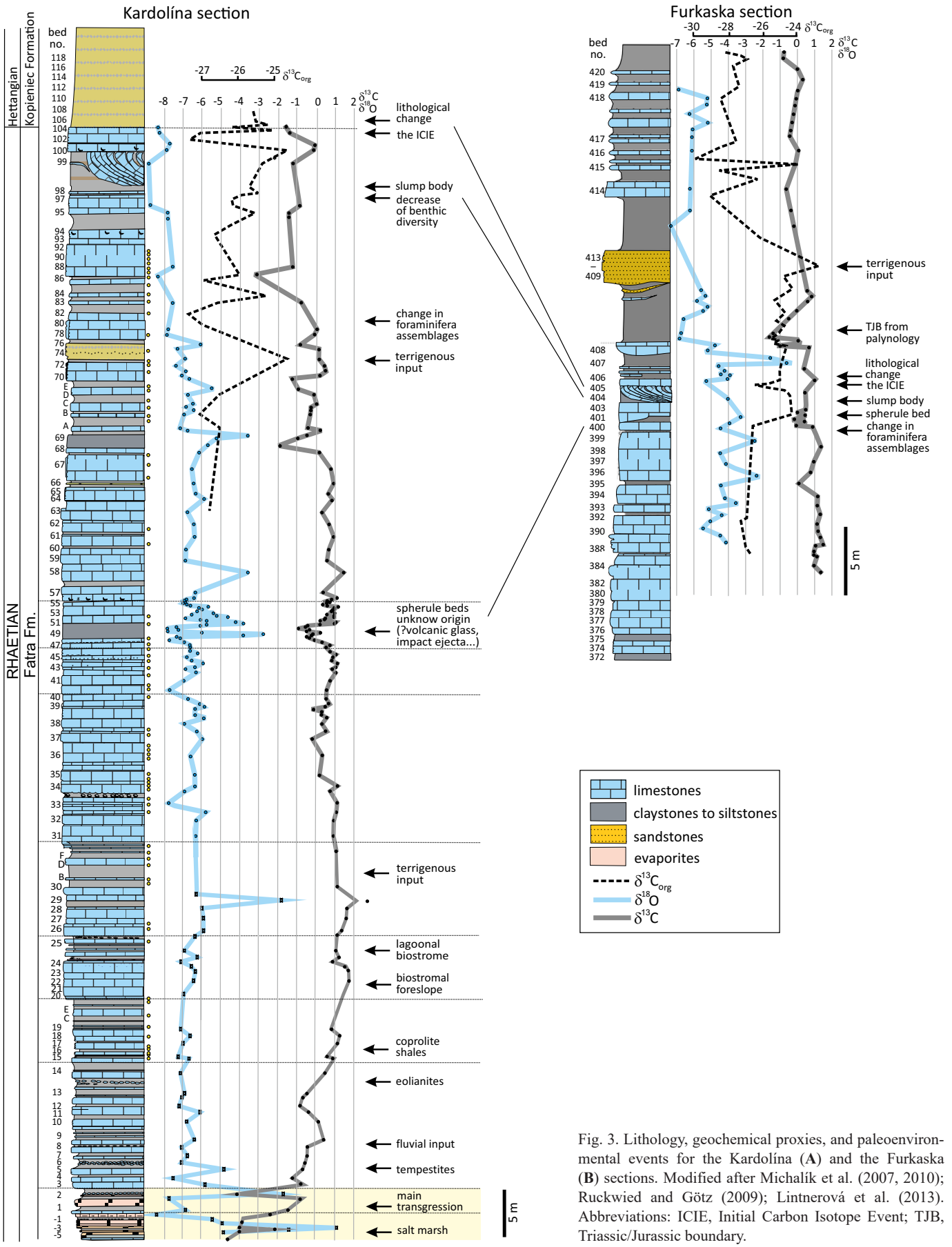

Fig. 3. Lithology, geochemical proxies, and paleoenvironmental events for the Kardolína (**A**) and the Furkaska (**B**) sections. Modified after Michalík et al. (2007, 2010); Ruckwied and Götz (2009); Lintnerová et al. (2013). Abbreviations: ICIE, Initial Carbon Isotope Event; TJB, Triassic/Jurassic boundary.

Beds 399–401 in the Furkaska section) just above the major isotope excursions (positive $\delta^{18}O_{inorg}$ peak and negative $\delta^{13}C_{org}$ excursion). Although the interpretation of their origin is unclear (impact ejecta, volcanic glass, or altered aragonite particles), they enable a correlation between the Furkaska and Kardolína sections. Slump bodies are of some correlation value, too. Submarine slumps are represented by Bed 98 in the Kardolína section and Bed 404 in the Furkaska section; in both cases immediately above the lithological changes represented by boundary claystone. Their position at the top of the Rhaetian sequence parallels that in other parts of the Carpathians but also elsewhere in Europe, e.g., in the Alps and in SW Britain (Hesselbo et al. 2004; Michalík et al. 2007). Submarine slumping phenomena indicate an enhanced tectonic activity, which was associated with the Late Triassic Extinction in Europe (Lindström et al. 2017).

A shift from carbonate sedimentation to clastic one indicates an enhanced terrigenous input due to accelerated runoff (Bed 105 of the Kardolína section and Bed 405 of the Furkaska section). Clay mineral analysis also suggests an increasing intensity of chemical weathering during periods of elevated humidity (mega monsoons), which resulted in the kaolinization during the Rhaetian–Hettangian (Michalík et al. 2010, 2013; Lintnerová et al. 2013). The sharp lithological change between the Fatra and the Kopieniec formations marks a sudden termination of carbonate sedimentation, followed by the deposition of non-carbonate boundary claystone. This is also a consequence of elevated humidity during the TJB interval, as described from several areas of Europe (Lintnerová et al. 2013 and references therein).

Another significant marker of the TJB is the palynological turnover recorded in the uppermost part of the Fatra Formation (Beds 408/409 in the Furkaska section). The change in the palynological association in favour of sporomorph dominance is interpreted as an effect of a sudden humidity increase (Ruckwied and Götz 2009).

The broader TJB interval is also marked by a change in foraminiferal assemblages, as documented by in Beds 78–80 in the Kardolína section and Beds 399–400 in the Furkaska section (Michalík et al. 2007).

Material and methods

The Kardolína section is located in the rocky slope (Husár Hill) of Mt. Pálenica above the Kardolína gamekeeper house near Tatranská Kotlina, Belá Tatra Mountains (49°15'00.0"N 20°18'53.4"E; Figs. 1, 2, geological situation modified from https://apl.geology.sk/). Its lithological and geochemical variations are summarized in Fig. 3.

The Furkaska section is located in a gorge on the slope of Mount Furkaska in the Juráňova Valley in the Western Tatra Mountains (49°16'17.4"N 19°46'12.0"E). Variations in lithology and geochemical data are illustrated in Fig. 3B.

In total, 168 calcareous nannoplankton samples acquired in two field campaigns were analysed. Of these, 109 came from the Kardolína section (96 from Fatra Formation and 13 from Kopieniec Formation) and 59 from the Furkaska section (22 from Fatra Formation and 37 from Kopieniec Formation; SOM 1, Supplementary Online Material available at http://app.pan.pl/SOM/app69-Holcova_etal_SOM.pdf). Extraction of calcareous nannofossils, due to their fragile structure, presents a challenge especially from ancient carbonate rocks. This research was also focused on the development of an extraction method from indurated rocks (like marine carbonates) and on sample enrichment.

Calcareous nannofossils were studied under a scanning electron microscope (SEM) and optical polarizing microscope. First, standard nannoplankton smear slides were inspected for the presence of calcareous nannofossils; samples with the most abundant nannofossils were chosen for the SEM study. For SEM analysis, nannoplankton samples were concentrated using the floating method (Švábenická 2002) and subsequently studied from a drop of floated suspension. Besides the drops of suspension from floated samples, rock fragments were also analysed by the SEM.

For the Kopieniec Formation, a modified preparation method was developed for nannofossil extraction. It is based on the method proposed by Minoletti et al. (2009), which enables an enhancement in relative abundances of nannoliths in consolidated rocks. It consists of a multi-staged apparatus (Fig. 4) that enables a continuous repeated wet vacuum-powered acoustic microfiltration. Primary suspension is sieved on a 10 μm sieve and, for a limited time, exposed to the ultrasonic cavitation. The top layers of the filtrate are transported to the sedimentation vessel via suction. Skimming interval of the top layer of the solution in the sedimentation vessel at the height mark was calculated from the terminal velocities for calcareous nannofossil-sized spherules and the retention time in the corresponding vessel, following the Stokes' law. The decanted solution was transported to the final vacuum filter flask with a pipette, after 15 minutes of sedimentation time. This novel approach was tested on 11 samples for which we postulated a high possibility of nannofossil occurrence. The high occurrence possibility results from the encountered lithological change where hard, lithified limestones give way to boundary clay and fine-grained disaggregated marls with higher clastic content. Lithological transition in the marls of the Kopienec Formation and the stratigraphical position minimized the need to crush the samples prior to the extraction hence also the breakage of nannofossil remains. To demonstrate the

Table 1. Semiquantitative expression of nannolith and organic matter abundance in nannoplankton slides.

Category		Coverage by organic matter of the field of view	Number of fields of view/1 nannolith
0	none	0	0
1	very rare	<10 %	0 –20
2	rare	10–25 %	5–20
3	common	25–50 %	1–5
4	abundant	>50%	<1

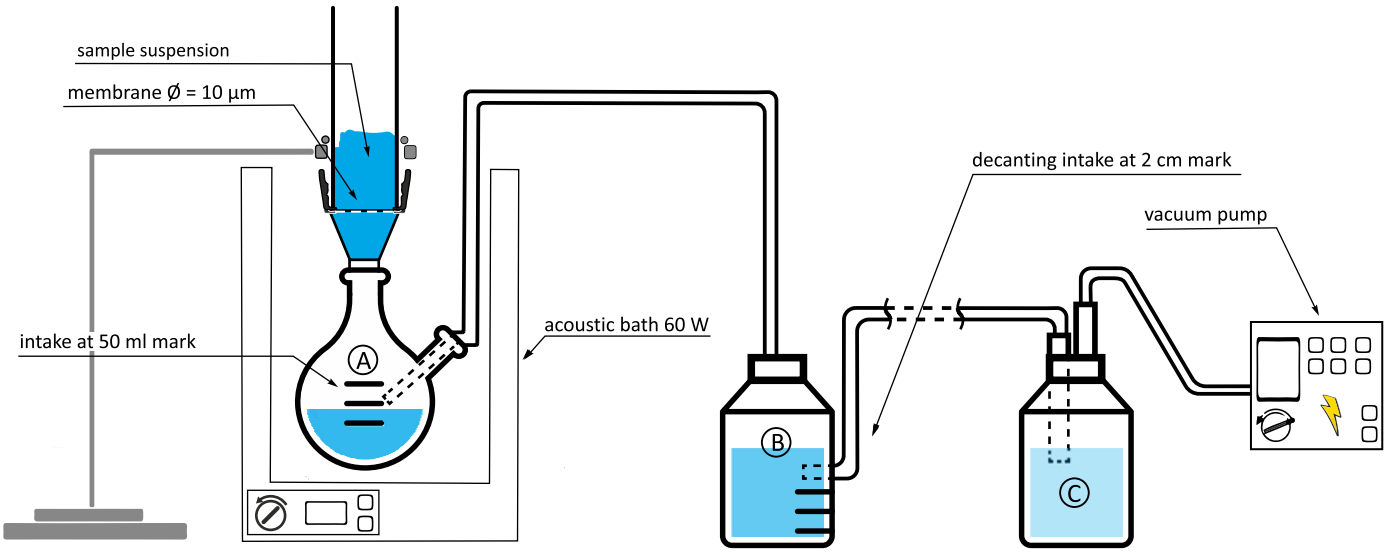

Fig. 4. Assembled device for repeated wet vacuum-powered filtration with automated decantation. Labels correspond to vessels at different stages of extraction and concentration. **A**. Collection of filtrate. **B**. Sedimentation vessel. **C**. Vacuum filter flask. Modified after Minoletti et al. (2009).

efficiency of the final operation of the new methodology, we present the resulting nannofossil abundances in per cent of change per 200 fields of view in comparison with samples where nannoplankton was extracted lower in the section using only the decanting method. The reason for utilizing only the decanting method lower in the section was the higher degree of lithification of the Fatra Formation limestones. Based on previous experience, the hard, competent limestones had a higher potential for progressive recrystallization, which made nannofossils more brittle and could have disturbed any palaeoecological signal.

The abundance of nannofossils in slides was expressed as number per field of view (counted for 200 fields of view from each sample). Taxonomically, however, we determined a maximum of 200 first nannoliths. Relative abundances of individual nannoplankton taxa were counted from at least 50 specimens (due to their scarcity). However, relative abundances of individual taxa counted from 50 to 200 specimens were considered as approximate estimates. The numbers of carbonate rhombohedra were counted by the numbers of nannofossils per field of view (counted for 200 fields of view from each sample; SOM 1) and expressed semiquantitative (Table 1).

Results

Efficacy of the new extraction method.—Efficacy of the modified extraction was evaluated based on a change in the numbers of nannofossils per 200 fields of view. This evaluation was performed from the standpoint of replicating the results obtained by Minoletti et al. (2009) using a similar approach but on a different device. The efficacy was tested on eleven samples, three of them contained no nannofos-

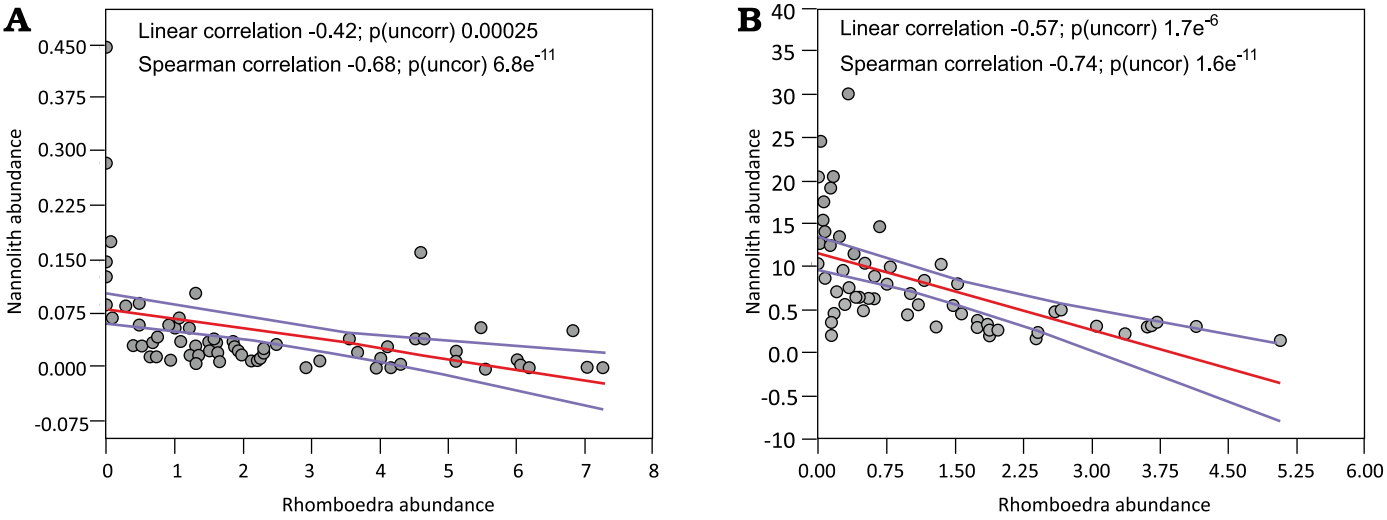

Fig. 5. A relation between the numbers of rhombohedra and the numbers of nannoliths per field of view of the microscope in the Triassic part of the Kardolína (**A**) and the Furkaska (**B**) sections.

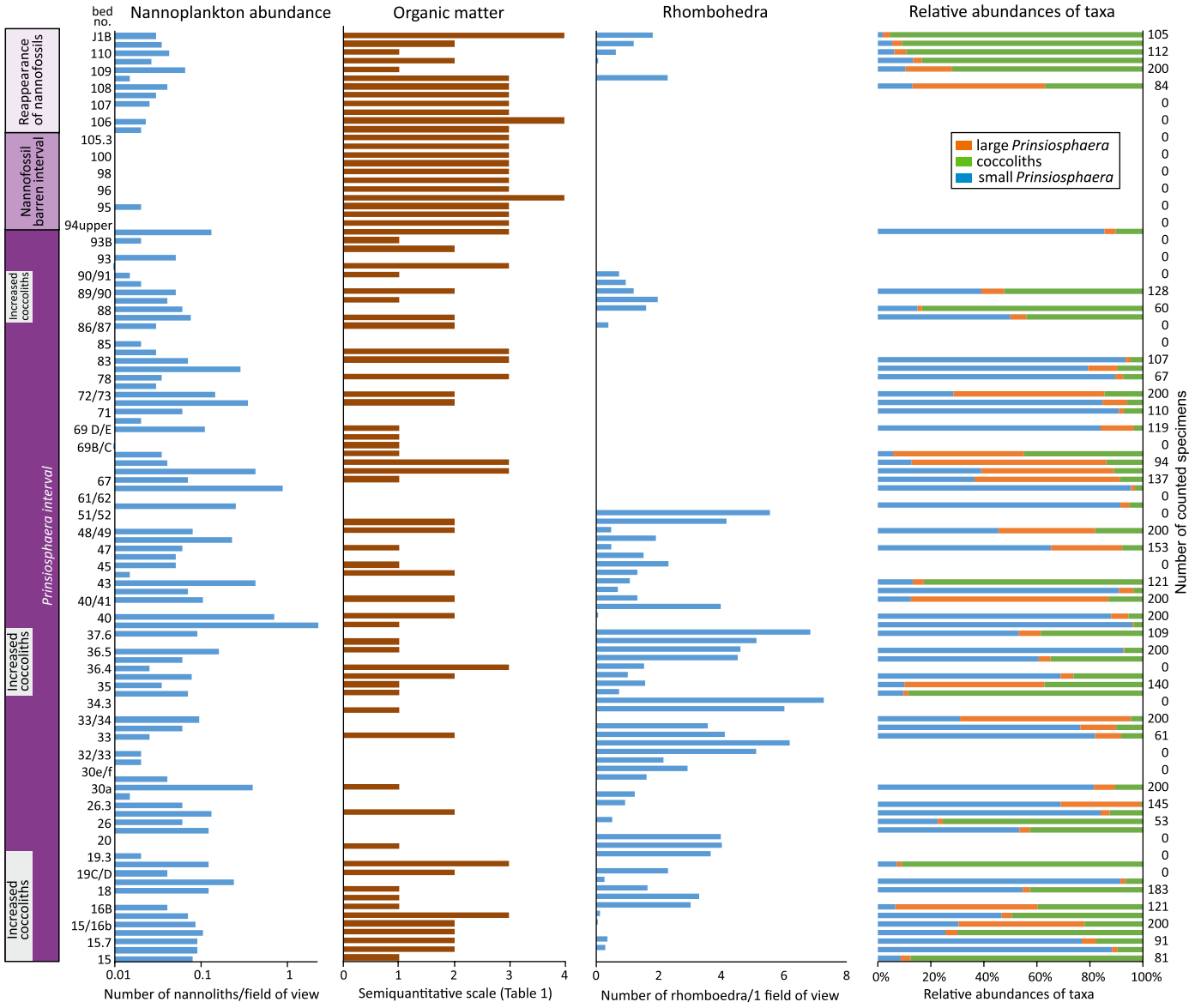

Fig. 6. Nannofossil quantitative results, semiquantitative amount of organic matter and numbers of rhombohedra obtained from the calcareous nannoplankton slides in the Kardolína section.

sils in simple smear slides and in smear slides prepared with the extraction method. In other samples, nannofossil abundances increased by ~60–70% (Table 2). Due to the small numbers of nannofossil specimens, the quantification of the increase in abundance is only approximate. Using the tested samples and a subsequent comparison with the control material, a general increase in the abundance of the assemblages was documented. This provides a final proof of the concept of the described modified extraction approach.

Characteristics of calcareous nannofossil assemblages.—Calcareous nannofossils are generally very rare (0.01–2.28 nannoliths per field of view) and of low diversity (eighteen taxa in total). The numbers of species per sample vary from one to seven (SOM 1). Nannofossil preservation is moderate to poor, exhibiting signs of dissolution and overgrowth. Due to this poor preservation, we expected to observe a diage-

Table 2. Changes in nannolith abundances expressed in numbers of nannoliths per microscope field of view in slides prepared before and after the application of the extraction method.

Sample	Abundace of coccoliths/200 fields of view		Abundance increase [%]
	no extraction	with extraction	
104.3	0	0	0
104.7	0	0	0
105.1	1	3	175
105.6	5	7	158
106.0	15	25	162
106.4	10	22	168
107.5	0	0	0
107.9	5	7	158
108.4	20	31	160
108.8	0	0	0
109.0	17	25	159

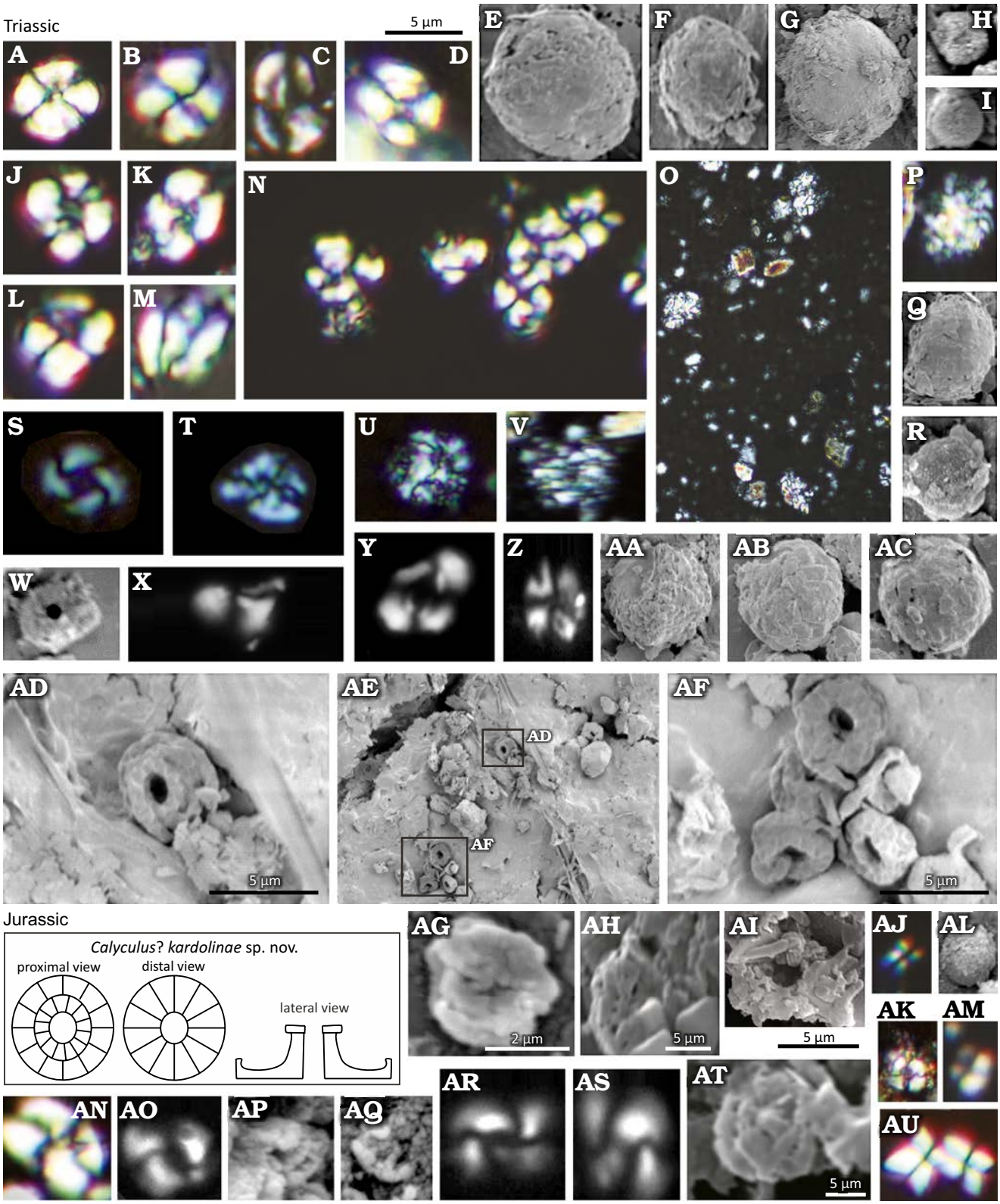

Fig. 7. Calcareous nannoplankton from the Kardolína section, Belá Tatra Mountains, Slovakia. **A–AF**. CHMHZ-KH-0003, Triassic. A, B, D, J–L, N, T, Coccolith 1; C, *Archaeozygodiscus* sp.; E–G, AA–AC, large-sized *Prinsiosphaera triassica* Jafar, 1983; H, I, small-sized *Prinsiosphaera triassica* Jafar, 1983; O–R, U–V, medium-sized *Prinsiosphaera triassica* Jafar, 1983; M, *Eoconusphaera* aff. *hallstattensis* Demangel et al. 2020; S, Coccolith 3; X, Y, Coccolith 2; W, a strongly recrystallized coccolith; AD–AF, *Calyculus*? *kardolinae* sp. nov. accumulated on a bedding plane (AD, holotype). **AG–AU**. CHMHZ-KH-0002, Jurassic. AG, Coccolith 6; AH, AI, AM, AP, AQ, AT, strongly recrystallized coccoliths; AJ, Nannolith Morphotype sp. 1 (Bottini et al. 2016); AK, AN, Coccolith 1; AL, small-sized *Prinsiosphaera triassica* Jafar, 1983; AO, AR, AS, Coccolith 4; AU, a *Tetralithus*-like structure. Scale bar above D applies to all except AD, AF, AG–AI, and AT.

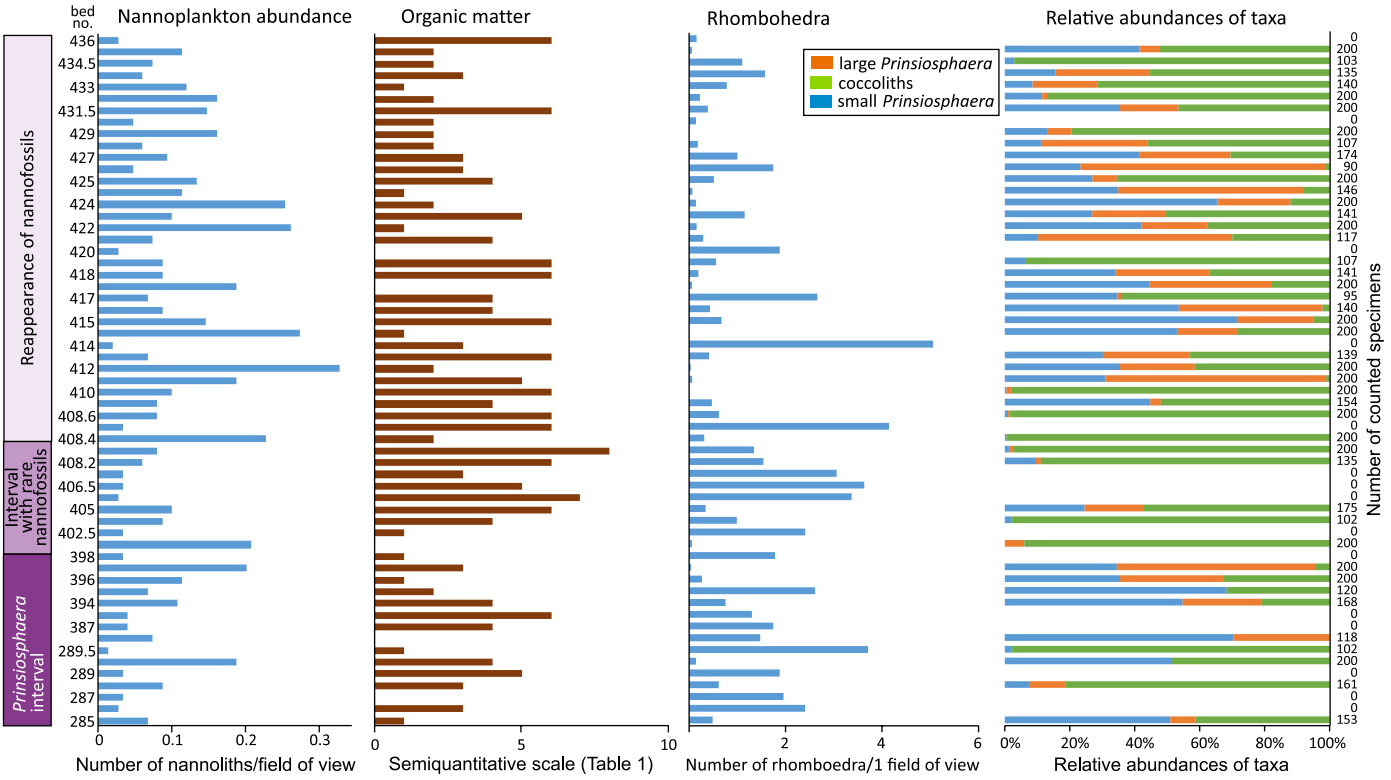

Fig. 8. Quantitative characteristics of calcareous nannoplankton assemblages, semiquantitative amount of organic matter and numbers of rhombohedra obtained from the calcareous nannoplankton slides in the Furkaska section.

netically driven decrease in nannofossil abundances. As a measure of the diagenetic recrystallization of carbonates, the number of carbonate rhombohedra per microscope field of view was taken. The statistically significant correlation between numbers of rhombohedra and numbers of nannofossils are illustrated in Fig. 5. This relation was supported by the test; statistically significant relations (p values of the tests <0.05) were obtained (Fig. 5). This indicates that the reduced numbers of nannofossils in the rock is controlled by diagenetic recrystallization associated with the formation of the rhombohedra.

Calcareous nannofossil events.—Kardolína section: Calcareous nannofossil assemblages from the Kardolína section can be divided into three intervals (Figs. 6, 7, Appendix 1). Samples from the lowermost interval of the section (Beds 0–15) were not studied for calcareous nannofossils because no nannofossils were expected due to the interpreted origin of carbonates in a hypersaline lagoon.

Prinsiosphaera interval (Beds 15–93, Fatra Formation, Rhaetian) is dominated by *Prinsiosphaera triassica* (Fig. 7E–I, O–R, U–V, AA–AC), with episodical occurrence and elevated numbers of small coccoliths (<5 µm) in Beds 15–20, 35–37 and 87–89. The relative abundances of small coccoliths increased from 0% to 20–100% in the mentioned intervals (SOM 1). These levels are characterized by the absence of environmental stress markers such as euryhaline indicators, terrigenous input and spherules. The coccoliths are recrystallized which makes their determination very difficult. Therefore, only an informal taxonomy could be applied, and we classified the morphotypes as Coccolith 1–6 (Appendix 1).

In the Triassic part of the section, Coccolith 1 is common (Fig. 7A, B, D, J–L, N, T) while coccoliths 2 and 3 (Fig. 7S, X–Y) were recorded only sporadically.

The variation in the ratio between small (<5 µm) and large *P. triassica* (>5 µm) cannot be explained by the variation in the studied sedimentological, mineralogical and geochemical proxies (Fig. 6). None of these proxies correlated with the ratio between small and large *P. triassica.*

The occurrence of *Eoconusphaera* aff. *hallstattensis* is consistent with the Late Triassic age (Fig. 7M; Bed 33). A new morphotype of coccolith was found in sample 37. It was described as *Calyculus*? *kardolinae* sp. nov. The coccoliths were recorded on bedding surfaces (Fig. 7AD–AF).

The nannofossil-barren interval (Beds 94–105, broader TJB, Fatra Formation) is characterized by continuously abundant contents of organic matter (Fig. 6). The top of the interval is connected with a lithological change from limestones of the Fatra Formation to fine clastics of the Kopieniec Formation. A slump body was recorded at around Bed 100,

Nannofossils reappeared in the Jurassic Kopienec Formation (Beds 105–115)). Due to the lithological monotony (calcareous siltstones to claystones), sampling was performed at intervals of ca. 0.5 m. Numerous dolomitic rhombohedra were observed in the interval of about one metre above the lithological boundary (0.8 m). With the decreasing number

of rhombohedra, first coccoliths were found together with ascidian spicules. Coccoliths of the *Prinsiosphaera* interval (Coccolith 1, Fig. 7AU) became rare while a new morphotype, Coccolith 4, became common, much like Coccolith 3 (Fig. 7AO, AR, AS). Several specimens were determined as Watznaueriaceae (Fig. 7AG). Unfortunately, the coccoliths are strongly recrystallized (Fig. 7AH, AT, AP, AQ), which prevents their more accurate determination using SEM. Triassic nannofossils resembling Morphotype sp. 1 described by Bottini et al. (2016; Fig. 7AJ) and small-sized *Prinsiosphaera* (Fig. 7AL) were found to be very rare, probably reworked from the Triassic. The first recrystallized and dissolved coccoliths observed under SEM come from a sample 2.4 m above the lithological boundary (sample 105). In the interval of 2.4–4.4 m (samples 106–107), the abundances of coccoliths, rhombohedra and aragonite needles increased. Five metres above the lithological boundary (sample 108), the high contents of organic matter decreased, and the coccoliths became even more abundant.

Furkaska section: The Furkaska section recorded the lowermost Jurassic interval in a higher thickness than the Kardolína section; however, these two sections show a similarity in the evolution of nannofossil assemblages (Figs. 8, 9, SOM 1: sheets Furkaska and Kardolina; Michalík et al. 2007, 2010; Ruckwied and Götz 2009; Lintnerová et al. 2013).

The *Prinsiosphaera* interval (Rhaetian, Fatra Formation, Beds 289–402) is dominated by *Prinsiosphaera triassica* with repeatedly increased numbers of small coccoliths (Beds 285–286 and 395–396). In contrast to the Kardolína section, the coccoliths are more abundant; this is expressed by different in the modus of this parameter (0.039 for Kardolína section and 0.073 for Furkaska section). Variations in the ratio between the abundances of small and large *P. triassica* were recorded but no correlation was observed in the variations in the studied sedimentological and geochemical characteristics, similarly to the Kardolína section (Fig. 8). A higher diversity of coccoliths (Fig. 9B, C, E–H, L, N) was recorded at the level of the FOs of seven foraminiferal species (Beds 399–400; Michalík et al. 2010). Unfortunately, the coccoliths are strongly recrystallized.

The interval with rare nannofossils (uppermost Rhaetian, Fatra Formation, Beds 402–405) can be characterized by the continuously higher contents of organic matter, although the increase is not so pronounced as in the Kardolína section. The interval starts just above the spherule beds. Similarly to the Kardolína section, the slump body and the ICIE were recorded in this interval (Fig. 3B), which we consider a correlation horizon.

The reappearance of common calcareous nannofossils correlates with the lithological change from the Fatra Formation to the Kopieniec Formation, similarly to the Kardolína section. The lithological boundary is immediately followed by the palynologically determined TJB which correlates with the appearance of relatively abundant calcareous nannofossils (between Beds 407/408; Ruckwied and Götz 2009). The common occurrence of *Watznaueria* sp. should be mentioned (Fig. 9Q, W, X, AB–AF, AV). Large nannoliths of ?*Schizosphaerella* sp. were found here. An unambiguous determination is not possible because the cross section of the specimen is elliptical and the determination of the arrangement of crystallites is prevented by the recrystallization (Fig. 9Z). The occurrence of small *Prinsiosphaera triassica* and *Crucirhabdus minutus* is presumably the effect of redeposition. Fragments of radiolarians were also recorded in this interval. Above Bed 410, the preservation of nannofossil becomes poor; it is therefore expected that the documented fossil record is incomplete.

Systematic palaeontology

Phylum Haptista Cavalier-Smith, 2003

Subphylum Haptophytina Cavalier-Smith, 2015

Class Prymnesiophyceae Christensen, 1962, emend. Cavalier-Smith, 1996

Order Podorhabdales Rood et al., 1971, emend. Bown, 1987

Family Calyculaceae Noel, 1973

Genus *Calyculus* Noel, 1973

Type species: *Calyculus cribrum* Noël, 1973; Toarcian, Fecocourt; France.

Calyculus? *kardolinae* sp. nov.

IFPNI: PFN003347.

Fig. 7AD–AF.

Etymology: From the Kardolína section.

Holotype: CHMHZ-KH-0003, holotype is situated in small rock fragment coated by gold. High, broad distal-shield composed of radial elements, a proximal-shield reduced to a narrow cycle of elements, central-area empty (Fig. 7AD).

Type locality: The Kardolína section near Tatranská Kotlina, Belá Tatra Mountains (49°15’00.0”N 20°18’53.4”E), Slovakia.

Type horizon: Beds 33–37 of the Kardolína section, Rheatian, Fatra Formation.

Material.—CHMHZ-KH-0003, small rock fragment coated by gold. All specimens on the surface of rock fragment (Fig. 7AD–AF).

Diagnosis.—A broad distal shield composed of radial, non-imbricating elements, the number of elements is only estimated at 14–16 due to recrystallization. The proximal shield is reduced to a simple, narrow circle of elements, with a moderately elevated rim. The central area is empty. Generic assignment is questionable.

Description.—Elevated elliptical placoliths, proximal shield reduced, rim elevation moderate, central-area empty. Diameter 3.5–5.0 μm (5.0 μm in the holotype).

Stratigraphic and geographic range.—The species was found only in Beds 33–37 of the Kardolína section, Rheatian, Fatra Formation, Slovakia.

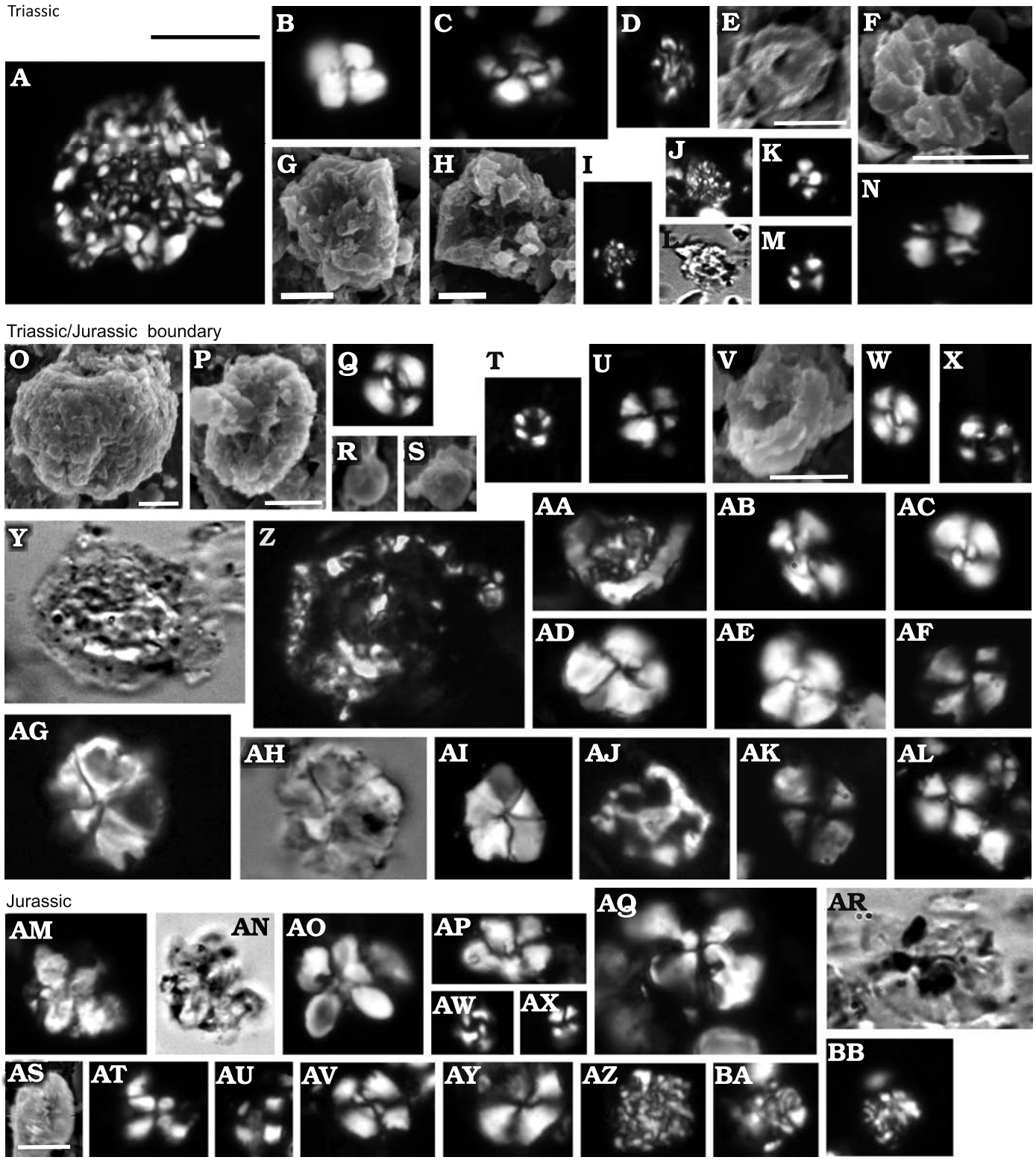

Fig. 9. Calcareous nannoplankton from the Furkaska section,Western Tatra Mountains, Slovakia (CHMHZ-KH-0001). **A**–**N**. Triassic. A, D, I, J, *Prinsiosphaera triassica* Jafar, 1983 (A, large; D, I, J small); B, Coccolith 1; C, Coccolith 2; E–H, L, N, strongly recrystallized coccoliths; K, M, Nannolith Morphotype sp. 1 (Bottini et al. 2016). **O**–**AL**. Triassic/Jurassic boundary. O, R, S, *Prinsiosphaera triassica* Jafar, 1983 (O, large; R, S, small); P, *Crucirhabdus* cf. *minutus* Rood et al., 1973; Q, W, X, AB–AF, Watznaueriaceae; T, Nannolith Morphotype sp. 1 (Bottini et al. 2016); U, V, strongly recrystallized and corroded coccoliths; Y, Z, Nannolith 1; AA, Chiastozygaceae cf. *Crepidolithus*; AG–AI, Nannolith 2; AJ, a holococcolith; AK, AL, Coccolith 4. **AM**–**BB**. Jurassic. AM–AO, AT, Nannolith 3; AP, AW, AY, Coccolith 2; AQ, AR, Coccolith 5; AS, a strongly overgrown coccolith; AU, AX, Nannolith Morphotype sp. 1 (Bottini et al. 2016); AV, Watznaueriaceae; AZ–BB, *Prinsiosphaera triassica* Jafar, 1983 (reworked). Scale bars 5 μm; scale bar above A applies to all except E–H, O, P, V, and AS.

Discussion

Correlation of calcareous nannoplankton, palynological, foraminiferal, sedimentological, and geochemical events.—The succession of events obtained from calcareous nannoplankton and multiproxy studies (Lintnerová et al. 2013; Michalík et al. 2007, 2010) was compared for the two studied sections (Fig. 10). The eventostratigraphic correlation of the Kardolína and Furkaska sections showed a similar succession of events in the latest Triassic (spherule beds, foraminifera turnover, disappearance/reduced abundance of nannoliths, slump body, ICIE). Common nannofossils reappear together with the lithological change followed by the appearance of the first Watznaueriaceae. The significant decrease in nannofossil abundances, frequently accompanied by an increase in organic matter, is considered to pose an ecostratigraphic event indicating the uppermost Triassic. Similarly to our sections, the decline in the abundance of Triassic nannofossils culminating during the initial negative Carbon Isotope Event was also recorded in the Lombardy Basin by Bottini et al. (2016). These authors associated the latest Triassic nannofossil decline with volcanism in the Central Atlantic Magmatic Province. This is also the assumption of the present authors. In our sections, this event can be correlated with the slump bodies formed in response to enhanced tectonic activity related to the ICIE and dated to 120 kyr prior to the TJB (Blackburn et al. 2013). Slumping structures are commonly found in the reworked carbonates. This represents gravitational transport triggered by high rates of sedimentation creating oversteepened slopes and by earthquakes (Flügel 2010). During the redeposition of the slump body, an increase in organic matter content can occur especially when combined with high rates of terrigenous sediment accumulation. The position of this ecostratigraphic event below the TJB is also supported by the appearance of the first Jurassic palynomorphs (Ruckwied and Götz 2009) just above this event.

Calcareous nannoplankton biostratigraphy.—Of the index species, only very rare *Eoconusphaera* aff. *hallstattensis* was recorded in the Zliechov Basin, which hampers the identification of its LO. However, it was recorded only in the Triassic part of the sections. Although species identification is uncertain, the genus became extinct at the end of the Triassic (Young et al. 2003). The LOs of *Prinsiosphaera triassica* and *Crucirhabdus minutus* are unclear probably due to the reworking of the Triassic nannofossils into Jurassic sediments.

Taphonomy of the calcareous nannoplankton fossil record around the TJB.—The poor preservation of nannofossils arises a question as to whether the decrease in the number of nannofossilsin the uppermost Triassic recorded in the Zliechov Basin reflects paleoecological patterns or rather diagenetic processes.

The impact of taphonomic processes on the composition of nannofossil assemblages could have been significant. The preservation of calcareous nannofossils indicates both diagenetic dissolution and overgrowth (Holcová and Scheiner 2023). A comparable preservation of nannofossils in this interval was recorded also by, e.g., Hillebrandt et al. (2013). However, the preservation of nannoplankton in this interval can be also better (e.g., Bottini et al. 2016).

A global paleoenvironmental effect can be expected in relation to the Central Atlantic Magmatic Province volcanic activity. Intensive carbonate dissolution was probably due to the reduced pH levels of seawater connected with this event (Felber et al. 2015; Lindström 2016). It has been proven by Erba (2006) and Bottini et al. (2016) that the Late Triassic disappearance of nannoplankton was induced by these events.

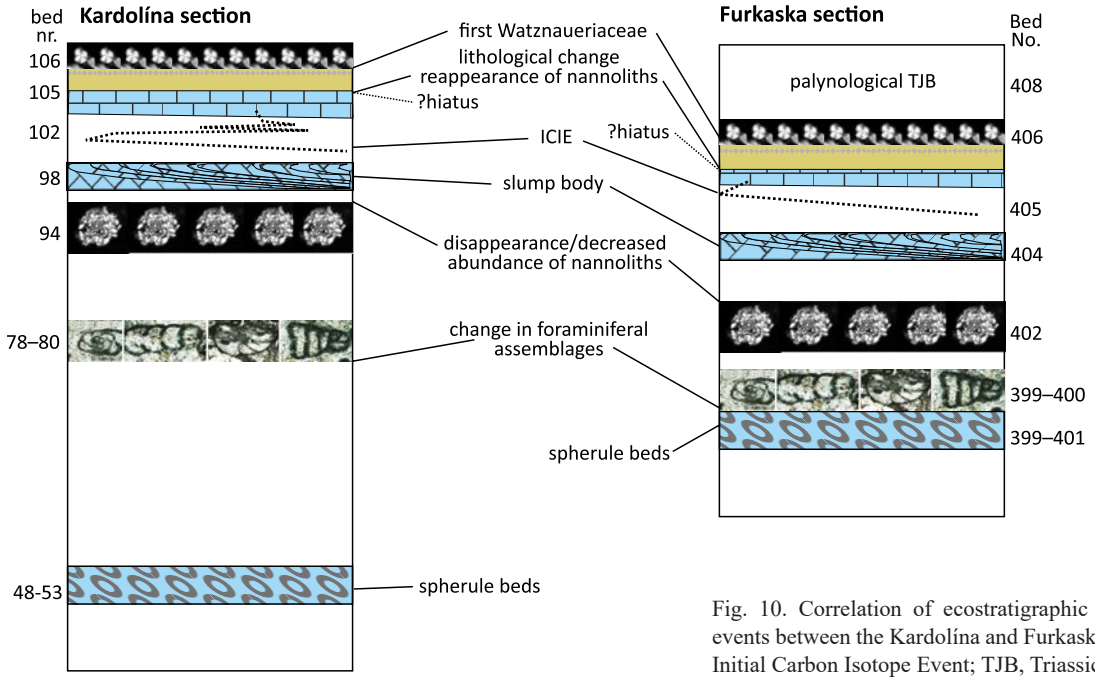

Fig. 10. Correlation of ecostratigraphic and calcareous nannoplankton events between the Kardolína and Furkaska sections. Abbreviations: ICIE, Initial Carbon Isotope Event; TJB, Triassic/Jurassic boundary.

The assemblages strongly dominated by *P. triassica* morphologically resemble the Paleogene and Neogene *Thoracosphaera* assemblages. As suggested by the observations in Miocene sediments, these assemblages may represent a dissolution relict of the original assemblages because laminae with well-preserved diversified nannofossils do episodically appear inside sequences dominated by *Thoracosphaera* spp. (Holcová et al. 2015; Kopecká et al. 2018). Then, morphologically similar *P. triassica* assemblages might represent dissolution relicts of the original assemblages, in which particularly small coccoliths were strongly affected. This interpretation is possibly supported by the observation that small coccoliths become more abundant in intervals where dolomitic rhombohedra, as a supposed product of recrystallization, are rare or almost missing (Fig. 5).

The monospecific calcareous nannoplankton assemblages may also indicate stress conditions which are expected at TJB. Such assemblages have been reported, among others, in connection with the collapse of nannoplankton production in Danian, just after the Cretaceous/Paleogene boundary (Gartner 1996; Latal 2004). Stress in surface seawater including a combination of changes in surface-water fertility and progressive ocean acidification has been interpreted for the TJB by Bottini et al. (2016). However, we did not record an increased production of smaller specimens of *P. triassica*, which was found in the Lombardy Basin.

In the case of a minimum impact of diagenetic dissolution on the calcareous nannoplankton assemblages, the herein identified repeated shifts between monospecific assemblages with *P. triassica* and assemblages with small coccoliths would imply a repeated alternation of favourable and stressful conditions in the upper part of the water column during the Rhaetian.

Conclusions

Calcareous nannofossil assemblages from the broader Triassic/Jurassic boundary interval were studied in the intra-shelf depression of the NW Tethyan shelf (Zliechov Basin), in sections of Kardolína and Furkaska.

Rhaetian assemblages are characterized by the dominance of *Prinsiosphaera triassica* and repeated increases in small coccolith abundances. The *P. triassica* assemblages might represent a dissolution relict of nannofossil assemblages or indicate stress condition in the surface seawater. Elevated abundances of small coccoliths probably indicate normal marine conditions and weaker diagenetic dissolution. Reduction in nannofossil abundances, frequently accompanied by an increase in organic matter, is considered to pose an ecostratigraphic event indicating the uppermost Triassic.

Rejuvenation of calcareous nannoplankton assemblages was recorded after the lithological change from the limestones to clastics, marked by the FOs of the first Jurassic palynomorphs. The appearance of the representatives of Watznaueriaceae already at the base of the Jurassic deposits may indicate a hiatus at the TJB in the studied sections.

The new extraction method was found to enhance nannofossil abundances in the slides.

Acknowledgements

We are very grateful for the constructive comments provided by Cinzia Bottini (Università degli Studi di Milano Statale, Italy) and two anonymous reviewers. This study was funded by the project COOPERATIO. We also acknowledge financial support of the VEGA Grant APVV-20-0079, 2/0090/19 and 2/0013/20.

References

Alroy, J. 2010. The shifting balance of diversity among major marine animal groups. *Science* 329: 1191–1194.

Blackburn T.J., Olsen P.E., Bowring S.A., McLean N.M., Kent D.V., Puffer J., McHone G., Rasbury E.T., and El-Touhami M. 2013. Zircon U-Pb geochronology links the end-Triassic Extinction with the Central Atlantic Magmatic Province. *Science* 340: 941–945.

Bonis, N.R. and Kürschner, W.M. 2012. Vegetation history, diversity patterns, and climate change across the Triassic/Jurassic boundary. *Paleobiology* 38: 240–264.

Borza, K., Gašparíková, V., Michalík, J., and Vašíček, Z. 1980. Upper Jurassic–Lower Cretaceous sequence of the Krížna Nappe (Fatric) in the Strážovce section, Strážovské vrchy Mts (Western Carpathians). *Geologicky Zborník Geologica Carpathica* 31: 541–562.

Bottini, C., Jadoul, F., Rigo, M., Zaffani, M., Artoni, C., and Erba, E. 2016. Calcareous nannofossils at the Triassic/Jurassic boundary: stratigraphic and paleoceanographic characterization. *Rivista Italiana Di Paleontologia E Stratigrafia* 122: 141–164.

Bown, P.R. 1985. *Archaeozygodiscus* gen. nov. and other Triassic coccoliths. *INA Newsletter* 7: 32–35.

Bown, P.R. 1987. The structural development of early Mesozoic coccoliths and its evolutionary and taxonomic significance. *Abhandlungen der Geologischen Bundesanstalt* 39: 33–49.

Bown, P.R. 1998. Triassic. *In*: P.R. Bown (ed.), *Calcareous Nannofossil Biostratigraphy. British Micropalaeontological Society Publication Series* 315: 29–33.

Bown, P.R., Burnett, J.A. and Gallagher, L.T. 1991. Critical events in the evolutionary history of calcareous nannoplankton. *Historical Biology* 5: 279–290.

Bralower, T.J., Bown, P.R., and Siesser, W.G. 1991. Significance of Upper Triassic nannofossils from the Southern Hemisphere (ODP Leg 122, Wombat Plateau, N.W. Australia). *Marine Micropaleontology* 17: 119–154.

Cavalier-Smith, T., Allsopp, M.T.E.P., Häuber, M.M., Gothe, G., Chao, E.E., Couch, J.A., and Maier, U.G. 1996. Chromobiote phylogeny: the enigmatic alga *Reticulosphaera japonensis* is an aberrant haptophyte, not a heterokont. *European Journal of Phycology* 31 (3): 255–263.

Cavalier-Smith, T. 2003. Protist phylogeny and the high-level classification of Protozoa. *European Journal of Protistology* 39 (4): 338–348.

Cavalier-Smith, T., Chao, E.E., and Lewis, R. 2015. Multiple origins of Heliozoa from flagellate ancestors: New cryptist subphylum Corbihelia, superclass Corbistoma, and monophyly of Haptista, Cryptista, Hacrobia and Chromista. *Molecular Phylogenetics and Evolution* 93: 331–362.

Christensen, T. 1962. Alger. *In*: T.W. Bscher, M. Lange, and T. Sorensen (eds.), *Botanik, Vol. 2. Systematisk botanik*, 1–178. Munksgaard, Copenhagen.

Deenen, M.H.L., Ruhl, M., Bonis, N.R., Krijgsman, W., Kuerschner, W.M., Reitsma, M., and van Bergen, M.J. 2010. A new chronology for the

end-Triassic mass extinction. *Earth and Planetary Science Letters* 291: 113–125.

Demangel, I., Kovács, Z., Richoz, S., Gardin, S., Krystyn, L., Baldermann, A., and Piller, W.E. 2020. Development of early calcareous nannoplankton in the late Triassic (Northern Calcareous Alps, Austria). *Global and Planetary Change* 193: 103254.

Dunhill, A.M., Foster, W.J., Azaele, S., Sciberras, J., and Twitchett, R.J. 2018. Modelling determinants of extinction across two Mesozoic hyperthermal events. *Proceedings of the Royal Society of London B* 285: 8.

Erba, E. 2006. The first 150 million years history of calcareous nannoplankton: Biosphere—geosphere interactions. *Palaeogeography, Palaeoclimatology, Palaeoecology* 232: 237–250.

Felber, R., Weissert, H.J., Furrer, H., Bontognali, and T.R.R. 2015. The Triassic–Jurassic boundary in the shallow-water marine carbonates from the western Northern Calcareous Alps (Austria). *Swiss Journal of Geosciences* 108, 213–224.

Flügel, E. 2010. *Microfacies of Carbonate Rocks, Analysis, Interpretation and Application*. 996 pp. Springer-Verlag, Berlin.

Gartner, S. 1996. Calcareous nannofossils at the Cretaceous–Tertiary boundary. *In*: N. MacLeod and G. Keller (ed.), *Cretaceous–Tertiary Mass Extinctions: Biotic and Environmental Changes*, 27–42 W.W. Norton, New York.

Gaździcki, A., Michalík, J., Planderová, E., and Sýkora M. 1979. An Upper Triassic–Lower Jurassic sequence in the Krížna Nappe (West Tatra Mts, Western Carpathians, Czechoslovakia). *Západné Karpaty, Geológia* 5: 119–148.

Goetel, W. 1917. Die rhätische Stufe und der unterste Lias der subtatrischen Zone in der Tatra. *Bulletin international de l'Académie des sciences de Cracovie: Classe des sciences mathématiques et naturelles*, *Séria A* (Supplement): 1–222.

Hallam, A. 1981. The end-Triassic bivalve extinction event. *Palaeogeography, Palaeoclimatology, Palaeoecology* 35: 1–44.

Hallam, A. and Wignall, P.B. 2000. Facies change across the Triassic–Jurassic boundary in Nevada, USA. *Journal of the Geological Society of London* 156: 453–456.

Hassenkam, T., Johnsson, A., Bechgaard, K., and Stipp, S.L. 2011. Tracking single coccolith dissolution with picogram resolution and implications for CO_2 sequestration and ocean acidification. *Proceedings of the National Academy of Sciences* 108: 8571–8576.

Hautmann, M. 2004. Effect of end-Triassic CO_2 maximum on carbonate sedimentation and marine mass extinction. *Facies* 50: 257–261.

Hautmann, M., Benton, M.J., and Tomašových, A. 2008. Catastrophic ocean acidification at the Triassic–Jurassic boundary. *Neues Jahrbuch für Geologie und Paläontologie Abhandlungen* 249: 119–127.

Hesselbo, S.P., Robinson, S.A., and Surlyk, F. 2004. Sea-level change and facies development across potential Triassic–Jurassic boundary horizons, SW Britain. *Journal of the Geological Society London* 161: 365–379.

Hillebrandt, A.V., Krystyn, L., Kürschner, W.M., Bonis, N.R., Ruhl, M., Richoz, S., Schobben, M.A.N., Urlichs, M., Bown, P.R., Kment, K., McRoberts, C.A., Simms, M., and Tomašových, A. 2013. The Global Stratotype Sections and Point (GSSP) for the base of the Jurassic System at Kuhjoch (Karwendel Mountains, Northern Calcareous Alps, Tyrol, Austria). *Episodes* 36: 162–198.

Holcová, K. and Scheiner, F. 2023. An experimental study on post-mortem dissolution and overgrowth processes affecting coccolith assemblages: A rapid and complex process. *Geobiology* 21: 193–209.

Holcová, K., Hrabovský, J., Nehyba, S., Hladilová, Š., Doláková, N., and Demeny, A. 2015. The Langhian (Middle Badenian) carbonate production event in the Moravian part of the Carpathian Foredeep (Central Paratethys): a multiproxy record. *Facies* 61: 419.

Jafar, S.A. 1983. Significance of late Triassic calcareous nannoplankton from Austria and Southern Germany. *Neues Jahrbuch für Geologie und Paläontologie Abhandlungen* 166: 218–259.

Jaraula, C.M.B., Grice, K., Twitchett, R., Böettcher, M., LeMetayer, P., Dastidar, A.G., and Opazzo, L.F. 2013. Elevated pCO_2 leading to End Triassic Extinction, photic zone euxinia and rising sea levels. *Geology* 41: 955–958.

Koiava, K., Mosar, J., Gavtadze, T., Kvaliashvili, L., and Mauvilly, J. 2015. Late Triassic Calcareous nannoplankton from Georgia and New Age of Moshevani Suite (Caucasus). *In*: Morard et al. (eds.), *Abstract Swiss Geoscience Meeting 2015 Platform Geosciences, Swiss Academy of Science, Stratigraphy*, 185–186.

Kopecká, J., Holcová, K., Nehyba, S., Hladilová, Š., Brzobohatý, R., and Bitner, M.A. 2018. The earliest Badenian *Planostegina* bloom deposit: reflection of an unusual environment in the westernmost Carpathian Foredeep (Czech Republic). *Geological Quarterly* 62: 18–37.

Kuss, J. 1983. Faziesentwicklung in proximalen Intraplattform-Becken: Sedimentation, Palökologie und Geochemie der Kössener Schichten (Ober-Trias, Nördliche Kalkalpen). *Facies* 9: 61–172.

Latal, C. 2004. The Cretaceous–Paleogene boundary section of Gorgo a Cerbara: an integrated stratigraphical study. *Annalen des Naturhistorischen Museums in Wien. Serie A für Mineralogie und Petrographie, Geologie und Paläontologie, Anthropologie und Prähistorie* 106: 259–279.

Lindström, S. 2016. Palynofloral patterns of terrestrial ecosystem change during the end-Triassic event—a review. *Geological Magazine* 153: 223–251.

Lindström, S., van de Schootbrugge, B., Hansen, K.H., Pedersen, G.K., Alsen, P., and Thibault, N. 2017. A new correlation of Triassic–Jurassic boundary successions in NW Europe, Nevada and Peru, and the Central Atlantic Magmatic Province: A time-line for the end-Triassic mass extinction. *Palaeogeography Palaeoclimatology Palaeoecology* 478: 80–102.

Lintnerová, O., Michalík, J., Uhlík, P., Soták, J., and Weissová, Z. 2013. Triassic–Jurassic climate humidification and Rhaetian kaolinite formation (Western Carpathians, Tatric Unit, the Červený Úplaz section). *Geological Quarterly* 57: 701–728.

Lowenstein, T.K., Timofeeff, M.N., Brennan, S.T., Hardie, L.A., and Demicco, R.V. 2001. Oscillations in Phanerozoic seawater chemistry: Evidence from fluid inclusions in salt deposits. *Science* 294: 1086–1088.

Marzoli, A., Bertrand, H., Knight, K. B., Cirilli, S., Buratti, N., Verati, C., Nomade, S., Renne, P. R., Youbi, N., Martini, R., Allenbach, K., Neuwerth, R., Rapaille, C., Zaninetti, L., and Bellieni, G. 2004. Synchrony of the Central Atlantic magmatic province and the Triassic–Jurassic boundary climatic and biotic crisis. *Geology* 32: 973–976.

Marzoli, A., Bertrand, H., Knight, K., Cirilli, S., Nomade, S., Renne, P., Verati, C., Youbi, N., Martini, R., and Bellieni, G. 2008. Comments on "Synchrony between the Central Atlantic magmatic province and the Triassic–Jurassic mass-extinction event?" by Whiteside et al. (2007). *Palaeogeography, Palaeoclimatology, Palaeoecology* 262: 189–193.

Marzoli, A., Jourdan, F., Puffer, J.H., Cuppone, T., Tanner, L.H., Weems, R.E., Bertrand, H., Cirilli, S., Bellieni, G., and De Min, A. 2011. Timing and duration of the Central Atlantic magmatic province in the Newark and Culpeper basins, eastern USA. *Lithos* 122: 175–188.

McElwain, J.C., Popa, M.E., Hesselbo, S.P., Haworth, M., and Surlyk F. 2007. Macroecological response of terrestrial vegetation to climatic and atmospheric change accross the Triassic/Jurassic Boundary in East Greenland. *Paleobiology* 33: 547–573.

Michalík, J. 1973. Paläogeographische Studie des Räts der Krížna Decke des Strážov Gebirges und einiger anliegender Gebiete. *Geologický zborník Geologica Carpathica* 24: 123–140.

Michalík, J. 1974. Zur Paläogeographie der rhätische Stufe des westlichen Teiles der Krížna Decke in der Westkarpaten. *Geologický zborník Geologica Carpathica* 25: 257–285.

Michalík, J. 1975. Genus *Rhaetina* Waagen, 1882 (Brachiopoda) in the uppermost Triassic of the West Carpathians. *Geologický zborník Geologica Carpathica* 26: 47–76.

Michalík, J. 1977. Paläogeographische Untersuchungen der Fatra-Schichten (Kössen Formation) des N Teiles des Fatrikums in den Westkarpaten. *Geologický zborník Geologica Carpathica* 28: 71–94.

Michalík, J. 1978. To the paleogeographic, paleotectonic and paleoclimatic development of the West Carpathian area in the uppermost Triassic. *In*: V. Vozár (ed.), *Paleogeographic Development of the Western Carpathians*, 189–211. Dionýz Štúr Geological Institute, Bratislava.

Michalík, J. 1980. A paleoenvironmental and paleoecological analysis of the northern Tethyan nearshore region in the latest Triassic time. *Rivista Italiana di Paleontologia e Stratigrafia* 85: 1047–1064.

Michalík, J. 1982. Uppermost Triassic short-lived bioherm complexes in the Fatric, Western Carpathians. *Facies* 6: 129–146.

Michalík, J. 1993. Mesozoic tensional basins in the Alpine-Carpathian shelf. *Acta Geologica Hungarica* 36: 395–403.

Michalík, J. 1994. Notes on the paleogeography and paleotectonics of the Western Carpathian area during the Mesozoic. *Mitteilungen der Osterreichishen Geologischen Gesellschaft* 86: 101–110.

Michalík, J. 2007. Sedimentary rock record and microfacies indicators of the latest Triassic to mid-Cretaceous tensional development of the Zliechov Basin (Central Western Carpathians). *Geologica Carpathica* 58: 443–453.

Michalík, J. and Jendrejáková, O. 1978. Organism communities and biofacies of the Fatra Formation (uppermost Triassic, Fatric) in the West Carpathians. *Geologický zborník Geologica Carpathica* 29: 113–137.

Michalík, J., Biroň, A., Lintnerová, O., Götz, A.E., and Ruckwied, K. 2010. Climatic change at the T/J boundary in the NW Tethyan Realm (Tatra Mts, Slovakia). *Acta Geologica Polonica* 60: 535–548.

Michalík, J., Lintnerová, O., Gaździcki, A., and Soták, J. 2007. Record of environmental changes in the Triassic–Jurassic boundary interval in the Zliechov Basin, Western Carpathians. *Palaeogeography, Palaeoclimatology, Palaeoecology* 244: 71– 88.

Michalík, J., Lintnerová, O., Wójcik-Tabol, A., Gaździcki, J., Grabowski, M., Golej, M., Šimo, V., and Zahradníková, B. 2013. Paleoenvironments during the Rhaetian transgression and the colonization history of marine biota in the Fatric Unit (Western Carpathians). *Geologica Carpathica* 64: 39–62.

Minoletti, F., Hermoso, M., and Gressier, V. 2009. Separation of sedimentary micron-sized particles for palaeoceanography and calcareous nannoplankton biogeochemistry. *Nature Protocols* 4: 14– 24.

Noël, D. 1973. Nannofossiles calcaires de sédiments jurassiques finement laminés. *Bulletin du Muséum National d'Histoire Naturelle* 75: 95–156.

Posch, F. and Stradner, H. 1987. Report on Triassic Nannoliths from Austria. *Abhandlungen der Geologischen Bundesanstalt in Wien* 39: 231–237.

Preto, N., Agnini, C., Rigo, M., Sprovieri, M., and Westphal, H. 2013a. The calcareous nannofossil *Prinsiosphaera* achieved rock-forming abundances in the latest Triassic of western Tethys: consequences for the $\delta^{13}C$ of bulk carbonate. *Biogeosciences* 10: 6053–6068.

Preto, N., Rigo, M., Agnini, C., Bertinelli, A., Guaiumi, C., Borello, S., and Westphal, H. 2012. Triassic and Jurassic calcareous nannofossils of the Pizzo Mondello section: a SEM study. *Rivista Italiana di Paleontologia e Stratigrafia* 118: 131–141.

Preto, N., Willems, H., Guaiumi, C., and Westphal, H. 2013b. Onset of significant pelagic carbonate accumulation after the Carnian Pluvial Event (CPE) in the western Tethys. *Facies* 59: 891–914.

Rakús, M. 1975. Hettangian ammonites from the Strážovská hornatina Mts. Západné Karpaty. *Paleontológia* 1: 7–23.

Rakús, M. 1993. Liassic ammonites of the Western Carpathians,1: Hettangian. Západné Karpaty. *Paleontológia* 17: 7–40.

Rakús, M. 2003. Hettangian ammonites in the Western Carpathians. *In*: J. Michalík (ed.), *IGCP 458: Triassic/Jurassic Boundary Events. Third Field Workshop, Stará Lesná, Slovakia*: 1–72. Veda, Bratislava.

Rood, A.P., Hay, W.W., and Barnard, T. 1971. Electron microscope studies of Oxford Clay coccoliths. *Eclogae Geologicae Helvetiae* 64: 245–272.

Ruckwied, K. and Götz, A.E. 2009. Climate change at the Triassic/Jurassic boundary: Palynological evidence from the Furkaska section (Tatra Mountains, Slovakia). *Geologica Carpathica* 60: 139–149.

Ruhl, M., Bonis, N.R., Reichart, G.J., Damsté, J.S.S., and Kürschner, W.M. 2011. Atmospheric carbon injection linked to end-Triassic mass extinction. *Science* 333: 430–434.

Stanley, S.M. 2006. Influence of seawater chemistry on biomineralization throughout Phanerozoic time: paleontological and experimental evidence. *Palaeogeography, Palaeoclimatology, Palaeecology* 232: 214–236.

Stanley, S.M. 2008. Effects of global seawater chemistry on biomineralization: past, present, and future. *Chemical Reviews* 108: 483–498.

Stur, D. 1859. Über die Kössener Schichten im nord-westlichen Ungarn. *Sitzungberichteder matematisch-naturwissenschaftlichen Classeder kaiserlichen Akademie der Wissenschaften* 38: 1006–1024.

Švábenická, L. 2002. Calcareous nannofossils of the Upper Karpatian and Lower Badenian deposits in the Carpathian Foredeep, Moravia (Czech Republic). *Geologica Carpathica* 53: 197–210.

Tanner, L.H., 2010. The Triassic isotope record. *In*: S.G. Lucas (ed.), The Triassic Timescale. *The Geological Society of London Special Publications* 334: 103–118.

Tetsuji, O., Michalík, J., Shirozu, H., Yamashita, M., Yamashita, K., Kusaka, S., and Soda, K. 2022. Extreme continental weathering in the northwestern Tethys during the end-Triassic mass extinction. *Palaeogeography Palaeoclimatology Palaeoecology* 594: 110934.

Tomašových, A. 2004. Microfacies and depositional environment of an Upper Triassic intraplatform carbonate basin: the Fatric Unit of the West Carpathians (Slovakia). *Facies* 50: 77–105.

Tomašových, A. and Michalík, J. 2000. Rhaetian/Hettangian passage beds in the carbonate development in the Krížna Nappe (central Western Carpathians, Slovakia). *Slovak Geological Magazine* 6: 241–249.

Vďačný, M., Michalík, J., and Lintnerová, O. 2019. Tectonic discrimination of siliciclastic sedimentary record of the northern Tethyan margin at the end of the Triassic. *Geological Quarterly* 63: 30–38.

Whiteside, J.H., Olsen, P.E., Eglinton, T., Brookfield, M.E., and Sambrotto, R.N. 2010. Compond-specific carbon isotopes from Earth's largest flood basalt eruptions directly linked to the end-Triassic mass extinction. *Proceedings of the National Academy of Sciences* 107: 6721–6725.

Whiteside, J.H., Olsen, P.E., Kent, D.V., Fowell, S.J., and Et-Touhami, M. 2007. Synchrony between the Central Atlantic magmatic province and the Triassic–Jurassic mass-extinction event? *Palaeogeography, Palaeoclimatology, Palaeoecology* 244: 345–367.

Wignall, P.B. 2001. Large igneous provinces and mass extinctions. *Earth Science Reviews* 53: 1–33.

Young, J.R., Bown, P.R., and Lees, J.A. 2023. *Nannotax3 website*. International Nannoplankton Association [available online, https://www.mikrotax.org/Nannotax3].

Appendix 1

List of calcareous nannofossil taxa/morphotypes.

Triassic and Jurassic

Prinsiosphaera triassica Jafar, 1983

Figs. 7E–I, O–R, U, V, AA–AC, AL, 9A, D, I, J, O, R, S, AZ–BB.

A broad variability in the size of specimens was observed (2–10 μm). Common to abundant in the Triassic; rare, reworked in the uppermost Jurassic.

Coccolith 1

Figs. 7A, B, D, J–L, N, T, AK, AN, 9B.

Elliptical coccoliths with a bar or a cross structure in the small central area and a bright rim visible in crossed polars.
Rare to common in the uppermost Triassic and lowermost Jurassic in both sections.

Coccolith 2

Figs. 7X, Y, 9C, AP, AW, AY.

Elliptical coccoliths with a closed to narrow central area and a bright rim visible in crossed polars with a thin, dark line in the middle of the rim.
Rare in the Triassic in the Kardolína section, common in the Triassic in the Furkaska section, common to abundant in the Jurassic.

Nannolith Morphotype sp. 1 (Bottini et al. 2016)

Figs. 7AJ, 9K, M, T, AU, AX.

Our morphotype resembles Morphotype sp. 1 of Bottini et al. (2016). It is a small nannolith (1 to 3 μm), composed of four elements that are blocky to ray-like.
Rare in the Triassic and Jurassic.

Tetralithus-like structure

Fig. 7AU.

Similar structures have been described as UFO 2 (Bown 1985), *Hayococcus floralis* Jafar, 1983 (Koiava et al., 2015), abraded *Tetralithus* sp. (Bottini et al., 2016). The structure may represent calcite rhombohedra or strongly recrystallized coccoliths.
Common mainly in the Furkaska section.

Triassic

Coccolith 3

Fig. 7S.

Coccoliths with dark external rims in crossed polars and with a closed central area.
The morphotype occurs very rarely only in the Kardolína section.

Eoconusphaera aff. *hallstattensis* Demangel, 2021

Fig. 7M.

Elliptical to subcircular conical nannofossils, truncated at both ends, with a flat to domed distal end. The outer mantle of elements is composed of tall, vertically orientated flat laths. The inner core is composed of a tall, thin element that is vertically to sub-vertically orientated. The exact determination is not possible due to poor preservation. Similar structures have been described as belonging to genus *Conusphaera* by Posch and Stradner (1987) and *Eoconusphaera* by Bottini et al (2016) and Demangel et al. (2020).
The morphotype was recorded only in Bed 33 of the Kardolína section.

Crucirhabdus cf. *minutus* Rood, Hay & Barnard, 1973

Fig. 9P.

Due to the strong overgrowth, detailed morphology of the rim cannot be studied. However, an axial cross is recognizable in the central area.
Very rare in the Triassic.

Archaeozygodiscus sp.

Fig. 7C.

A small coccolith with a rim formed of an outer/upper cycle, manifested by a dark line on the edge of the coccolith. A transverse bar occurs in the central part.
The morphotype occurs rarely in both sections in the Triassic.

Jurassic

Coccolith 4

Figs. 7AS, AR, AO, 9AK, AL.

Coccoliths with dark external rims in crossed polars and with a narrow central area.
The morphotype occurs rarely in both sections.

Coccolith 5

Fig. 9AQ, AR.

A large, circular coccolith with a closed central area and a dark external rim.
The morphotype was recorded only in the Furkaska section.

Coccolith 6

Fig. 7AG.

A small coccolith with distal and proximal shields and with a small central area with a diagonal cross.
One specimen in the Jurassic of the Kardolína section.

Watzenaueriaceae

Fig. 9Q, W, X, AB–AF, AV.

Coccoliths with a narrow central area, a bright rim and a thin, dark line inside the rim in crossed polars.
Rare in the Kardolína section, common in the Furkaska section.

Chiastozygaceae cf. *Crepidolithus* sp. or spp.

Fig. 9AA.

Coccoliths with broad, massive rims, bright in polarized light. The central area probably filled by a plate with a spine.

Nannolith 1

Fig. 9Y, Z.

Large, elipsoidal nannoliths, which may resemble compressed *Schizosphaerella* sp. The crystallite structure cannot be determined due to recrystallization; it is characteristic for genus *Schizosphaerella* (geometric arrangement of equidimensional crystallites).
One specimen was found in the Furkaska section.

Nannolith 2

Fig. 9AG–AI.

An irregular, pentagonal nannolith formed by 5 blocks of different shape. Light blocks prevail but one block may be dark in crossed polars.
The morphotype occurs rarely only in the Furkaska section.

Nannolith 3

Fig. 9AM–AO, AT.

Cubiform to slightly conical nannoliths composed of short, massive rays.
The morphotype occurs only in the Furkaska section.

Holococcolith

Fig. 9AJ.

A cavate holococcolith with a distinct conical central septum.
The morphotype occurs rarely only in the Furkaska section.